Geosciences and Engineering, Vol. 13, No. 1 (2025), pp. 5–15.
https://doi.org/10.33030/geosciences.2025.01.001

INFLUENCE OF FEEDSTOCK COMPOSITION ON THE ADSORPTIVE PROPERTIES OF RDF-BASED ACTIVATED CARBON

EMESE SEBE[1]*, JOHN KWAME BEDIAKO[2], YOUSSEF EL OUARDI[3], GÁBOR NAGY[4]

*[1]*Institute of Energy, Ceramic and Polymer Technology, University of Miskolc, emese.sebe@uni-miskolc.hu*
[2]Department of Separation Science, School of Engineering Science, Lappeenranta-Lathi University of Technology (LUT), FI-53850, Lappeenranta, Finland; john.bediako@lut.fi
[3]Department of Separation Science, School of Engineering Science, Lappeenranta-Lathi University of Technology (LUT), FI-53850, Lappeenranta, Finland; youssef.el.ouardi@lut.fi
[4]Institute of Energy, Ceramic and Polymer Technology, University of Miskolc, gabor.nagy2@uni-miskolc.hu
[1]ORCID 0000-0003-4797-4024
[2]ORCID 0000-0003-1816-4890
[3]ORCID 0000-0002-3199-0006
[4]ORCID 0000-0003-3571-9122

Abstract: This study focuses on converting refuse-derived fuel mixtures (composed of PS, PP, HDPE, paper, cardboard, cotton, and wood) into activated carbon through pyrolysis at 520 °C. The resulting chars underwent steam gasification at 900 °C for 60 min, with a steam flow rate of 5 $cm^3\ h^{-1}$. The physically activated chars were then systematically examined for their efficacy in removing phenol from 20 mg dm^{-3} solutions. The study demonstrated that the produced chars exhibited approximately half of the phenol removal efficiency of commercial activated carbon. Furthermore, an increased plastic content in the RDF blend enhanced the adsorption performance of the resulting activated carbons.

***Keywords**: activated carbon, refuse-derived fuel, adsorption, phenol, gasification, pyrolysis*

1. INTRODUCTION

Among the various adsorbent materials, activated carbons are widely utilized in water and gas purification. Approximately 100,000 tonnes of activated carbon are produced annually (Heidarinejad et al., 2020). One characteristic that stands out compared to zeolites and polymer-based adsorbents is their resistance to toxic and corrosive environments. The most common raw materials for activated carbon production include wood, bituminous coal, lignite, and coconut. However, there is an increasing demand for utilizing various wastes as raw materials (Heidarinejad et al., 2020).

Globally, more than 2.2 billion tonnes of municipal solid waste is generated each year and it is expected to reach 3.9 billion tonnes by 2050 (Liu et al., 2024).

Municipal solid waste is rich in carbonaceous materials; therefore, it could serve as an alternative raw material for activated carbon production. The challenge with this waste lies in its heterogeneous and variable nature. However, the fluctuations in its characteristics can be significantly reduced through mechanical processing, such as converting it into refuse-derived fuel (RDF).

The production of activated carbon involves two main steps: carbonization and activation. Activation can be achieved through physical methods, chemical methods, or impregnation (Thapar Kapoor et al., 2021). When physical activation is conducted using steam, an additional product is generated, i.e., synthesis gas (syngas). This gas primarily comprises hydrogen and carbon-monoxide and may find application in the chemical industry.

In this study, activated carbons were produced under laboratory conditions using RDF mixtures with varying compositions, and their phenol adsorption capacities were investigated. Phenol was selected as the adsorbate due to its prevalence as the main component of effluents from biomass gasification. Additionally, phenolic wastewater is commonly generated across various industrial sectors, including polypropylene production, oil refineries, and the paper, pharmaceutical, and textile industries (Cunha and Aguiar, 2014; Hernández-Fernández et al., 2021; Ke et al., 2022; Wang et al., 2022).

2. MATERIALS AND METHODS

2.1. Base material

The seven different materials investigated, which are commonly found in municipal waste, can be grouped into two categories, i.e., cellulosic materials (cardboard, paper, wood, cotton) and plastics (PS, PP, HDPE) (Figure 1).

Figure 1
Base components of RDF mixtures (1. cardboard, 2. office paper, 3. wood, 4. cotton, 5. PP, 6. PS, 7. HDPE)

Using the seven components presented above, model laboratory RDF mixtures with varying compositions were prepared, as shown in Table 1. The composition of RDF1 is based on an analysis of an RDF sample from a production plant in Hejőpapi, Hungary (Ladányi, 2015). A minor adjustment was made by excluding polyethylene terephthalate (PET), as there is an existing technology capable of effectively removing this component. This step was deemed necessary for two reasons: firstly, by separating PET, it becomes available for recycling; secondly, the pyrolysis of PET can pose challenges, such as the formation of benzoic acid, which can lead to system blockages and potential organic acid pollution (Xayachak et al., 2022). In the RDF2 and RDF3 samples, the total plastic content was increased by 10% and 20% by weight, respectively.

Table 1

Composition of RDF mixtures [wt.%]

Component	RDF1	RDF2	RDF3
Cardboard	9.00	7.76	6.52
Office paper	49.50	42.67	35.84
PP	5.50	7.50	9.50
HDPE	16.50	22.50	28.50
PS	5.50	7.50	9.50
Wood	10.00	8.62	7.24
Cotton	4.00	3.45	2.90

2.2. Activated carbon preparation

The experimental systems are depicted in Figure 2. The RDF mixture was subjected to pyrolysis at 520 °C with a heating rate of approximately 3.5 °C min^{-1}. The pyrolysis temperature was selected based on prior thermogravimetric analysis. Pyrolysis was conducted in a laboratory pyrolysis reactor equipped with electric heating. The material was placed in a 1 dm^3 beaker inside the reactor. After leaving the reactor, the pyrolysis gas passed through a heat exchanger, and the condensed liquid was collected in a glass vessel. The pyrolysis gases were also collected in a multi-layer gas sampling bag and subsequently analyzed using an Agilent 490 Micro GC gas chromatograph.

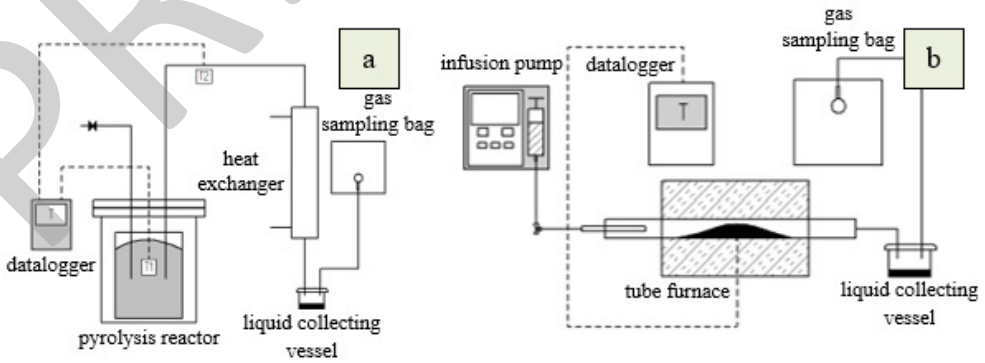

Figure 2

Laboratory pyrolysis (a) and gasification (b) systems

The resulting pyrolysis chars were then subjected to steam gasification at 900 °C for 1 h, with a heating rate of 10 °C min^{-1} and a steam flow rate of 5 cm^3 h^{-1}. These parameters were optimized in a prior study (Sebe et al., 2024). The steam activation of the chars was carried out in a laboratory gasification system, consisting of a tube furnace, a stainless-steel tube, and an infusion pump.

2.3. Adsorption experiments

The adsorption experiments were conducted using simulated phenol solutions with an initial concentration of 20 mg dm^{-3}. A total of 100 mg of activated carbon was added to 100 mL of the solution, and the mixtures were agitated on a reciprocal shaker. After 40 h, the mixtures were filtered, and the residual phenol concentrations were determined according to the ISO 6439:1990 standard titled, *"Water quality — Determination of phenol index — 4-Aminoantipyrine spectrometric method after distillation"*. Activated carbon from Thermo Fisher Scientific with a particle size of ≤ 2 mm and an iodine number of 969 mg g^{-1} was used as a reference point for the experimental evaluations.

The time required to reach adsorption equilibrium was determined using an initial solution concentration of 20 mg dm^{-3}. Pseudo-first-order (1) and pseudo-second-order (2) kinetic models were used to fit the data points.

$$q_t = q_e(1-e^{K_1 \cdot t}) \tag{1}$$

$$q_t = \frac{K_2 \cdot t \cdot q_e^2}{1+q_e \cdot K_2 \cdot t} \tag{2}$$

In these equations, q_e represents the equilibrium adsorption capacity (mg g^{-1}), q_t is the adsorption capacity at time t (mg g^{-1}), K_1 is the Lagergren first-order rate constant (1 min^{-1}), and K_2 is the Lagergren second-order rate constant (g min^{-1} mg^{-1}).

3. Results and Discussion

3.1. Pyrolysis behavior of RDF mixtures

The first step in the preparation of activated carbons was the pyrolysis of RDF mixtures. After each pyrolysis experiment, the weight of the produced chars was measured. Typically, during the degradation of most plastics, the predominant product is oil, resulting in less char compared to cellulosic and lignocellulosic materials. Consequently, increasing the plastic content of the RDF leads to a decrease in the amount of char produced. In this instance, the reduction occurred from 29.6 ± 0.1 to 24.6 ± 0.5 wt.%.

The composition of the gases produced during the carbonization process was analyzed by using a gas chromatograph capable of identifying hydrogen, carbon monoxide, methane, carbon dioxide, ethene, and ethane. Figure 3 illustrates the variation

of gas composition during pyrolysis of the experimental RDF blends as a function of the total PP, PS and HDPE content (27.5–47.5 wt.%) of the RDF.
With this method, 71.0–76.6 vol.% of the gases was identified, while the remaining portion possibly consisted of other hydrocarbons. Since the polymeric components of the RDF, apart from the additives, consist primarily of carbon and hydrogen atoms, increasing the plastic content in the RDF mixtures predictably resulted in a higher proportion of hydrocarbons in the produced gas. In contrast, increasing the proportion of cellulosic and lignocellulosic components in the RDF led to a greater presence of oxygen-containing gas components, such as CO_2.

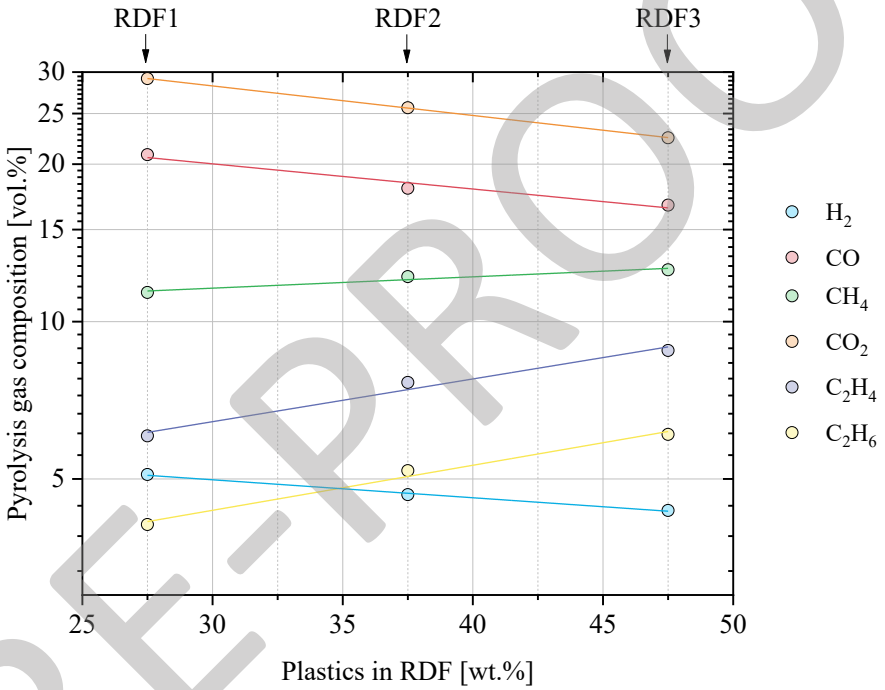

Figure 3
Composition of pyrolysis gases

Due to a significant portion of the produced gas remaining unidentified, it was not possible to accurately calculate its heating value. However, the trends shown in Figure 3 indicate that a higher plastic content in the RDF correlates with an increase in the heating value of the produced gas.

The results of experiments performed with a fixed PP:PS:HDPE ratio of 1:1:3 showed a linear relationship between the amount of plastic in the RDF and the proportion of each pyrolysis gas component. This linear relationship was strongest for H_2 (R^2=0.995) and CO_2 (R^2=0.999), and weakest for CH_4 (R^2=0.952), according to the coefficients of determination, R^2 values.

3.2. Characterization of RDF-based activated carbons

Table 2 presents the ultimate analysis of the RDF1-3 activated carbon samples. The most notable difference is observed in the carbon content, which increases as the ratio of plastic components in the initial RDF mixture increases.

Table 2

Ultimate analysis of activated RDF-chars [wt.%]

Sample	RDF1	RDF2	RDF3
Ultimate analysis (wt.%)			
C	48.4	51.5	53.4
H	1.1	1.1	1.2
N	<0.3	<0.3	<0.3
S	<0.2	<0.2	<0.2
O (by diff.)	0.0	0.0	0.0
Ash	50.5	47.4	45.4
LHV (kJ kg-1)	16636.0	16814.9	17956.2

Nitrogen physisorption measurements were performed under isothermal conditions, and the resulting adsorption and desorption isotherms are depicted in Figure 4, revealing distinct hysteresis loops. These loops are common in materials with mesopores and indicate capillary condensation (Das et al., 2024). According to the International Union of Pure and Applied Chemistry (IUPAC) classification, an H3-type loop can be seen here, which suggests slit-shaped pores (Bläker et al., 2019).

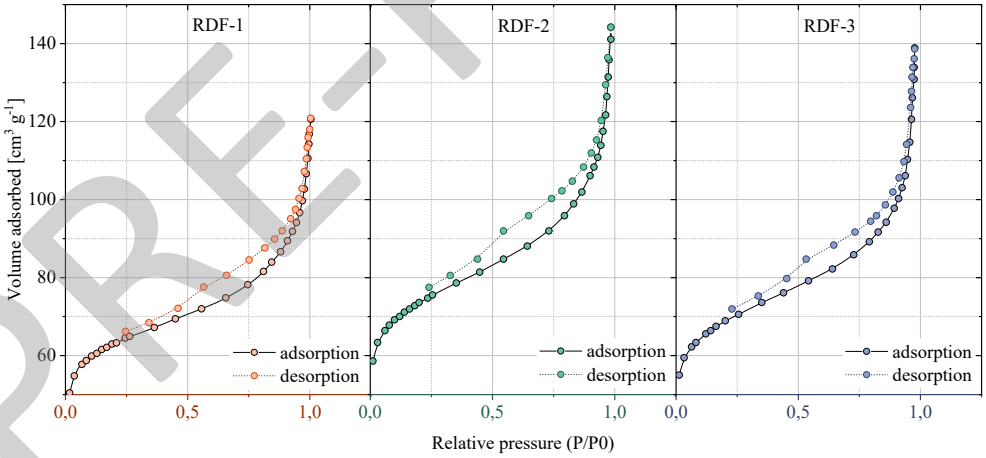

Figure 4

Adsorption and desorption isotherms of RDF chars

The gas adsorption analysis results are presented in Table 3. The specific surface area determined by the Brunauer–Emmett–Teller (BET) method, as well as the pore area and volume, reached their peak values for the RDF2 sample. This observation

aligns with findings from Adeniyi et al. (Adeniyi et al., 2024), who noted a synergy in biomass-plastic mixtures leading to the production of biochar with a higher specific surface area compared to biochar produced solely from biomass. It is possible that a similar synergy occurred in this study, suggesting that the optimal biomass-plastic ratio was achieved with RDF2.

Table 3

Gas adsorption analysis of RDF chars

Parameter	Unit	RDF1	RDF2	RDF3
BET, meas.	$m^2\ g^{-1}$	212.8	248.5	233.6
Total pore area	$m^2\ g^{-1}$	136.8	153.5	142.25
Total pore vol.	$m^3\ g^{-1}$	0.0631	0.0709	0.0658
Avr. pore diam.	nm	3.313	3.372	3.426

3.3. Phenol adsorption

The time dependence of phenol adsorption on RDF-based activated carbons was evaluated using an initial phenol concentration of 20 mg dm^{-3}. The results of adsorption experiments are presented in Figure 5. Increasing the initial plastic content of the RDF led to a corresponding increase in the adsorptive capacity of the resulting activated carbon.

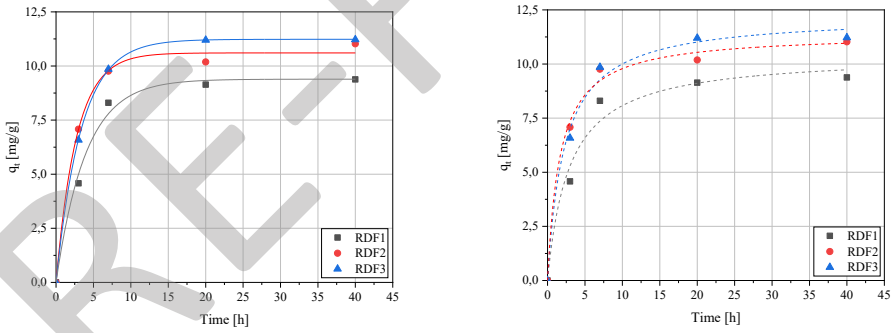

Figure 5

Time dependence of phenol adsorption on RDF-based activated carbons (PFO on the left and PSO on the right)

Table 4 summarizes the key parameters of the fitted pseudo-first order and pseudo-second order kinetic models. Based on the determination coefficient, the PFO model provided a better fit. Evaluating the adsorption efficiency of activated carbons derived from individual components, an estimated uptake capacity (q_{est}) was calculated for the RDF1–3 chars.

Table 4

Parameters of kinetic models fitted to the measurement points of RDF-based activated carbons

	Pseudo-first order			Pseudo-second order		
Par.	q_e	k_1	R^2	q_e	k_2	R^2
Unit	*mg/g*	*1/min*	-	*mg/g*	*mg/(g·min)*	-
RDF1	9,39 ± 0,28	0,25 ± 0,03	0,9903	10,45 ± 0,76	0,03 ± 0,01	0,9689
RDF2	10,60 ± 0,23	0,37 ± 0,03	0,9943	11,42 ± 0,38	0,05 ± 0,01	0,9920
RDF3	11,23 ± 0,02	0,30 ± 0,00	0,9999	12,25 ± 0,48	0,04 ± 0,01	0,9897

This estimation assumes no synergy between the components. Equation (3) outlines the calculation, where q_{est} represents the estimated value of phenol uptake capacity (wt.%), a_i (wt.%) denotes the ratio of the "i" component in the initial RDF mixture, r_i (wt.%) stands for the weight ratio of the remaining char during the pyrolysis of the "i" component, q_i (wt.%) indicates the uptake capacity of the activated carbon derived from component "i", and r_{RDF} (wt.%) represents the remaining char ratio of the RDF mixture.

$$q_{est} = \Sigma \frac{a_i \cdot r_i \cdot q_i}{r_{RDF} \cdot 100} \quad (3)$$

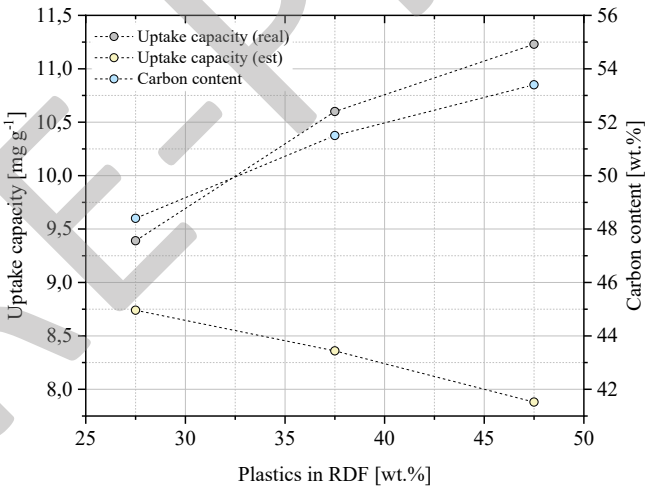

Figure 6

Estimated and real adsorption efficiency

This uptake capacity value specifically applies to the investigated conditions: a 20 mg dm^{-3} initial phenol concentration and a 1:1 (mg:mL) adsorbent-solution ratio.

Figure 6 compares the estimated and actual adsorptivity values, along with the carbon content, as a function of the total plastic content in the initial RDF blend. Contrary to expectations, an inverse trend was observed.

In other words, increasing the plastic content of the RDF resulted in improved adsorption efficiency. This could be due to a synergistic effect offered by the increasing presence of plastic in the RDF (Adeniyi et al., 2024). In the same conditions, the efficiency of RDF-based activated carbons is approximately 50–59% when compared to a commercial (Thermo Fisher) activated carbon. Unlike the specific surface area, the carbon content of the chars exhibited a stronger correlation with the uptake capacity. The surface area, pore size and carbon content all play crucial roles in the overall adsorptive capacity of activated carbons. Thus, the increasing adsorption efficiency trend from RDF1-3 could be attributed to factors such as the carbon content and average pore diameter rather than the surface area.

3.4. Examination of the by-product syngas

During the physical activation of the RDF-chars, an additional value-added product was generated, the synthesis gas. This gas was collected, and the composition analyzed using gas chromatography. The results of the gas analysis, along with the specific gas production, are presented in Figure 7. As the initial plastic content in the RDF blend increased, the overall gas production gradually decreased.

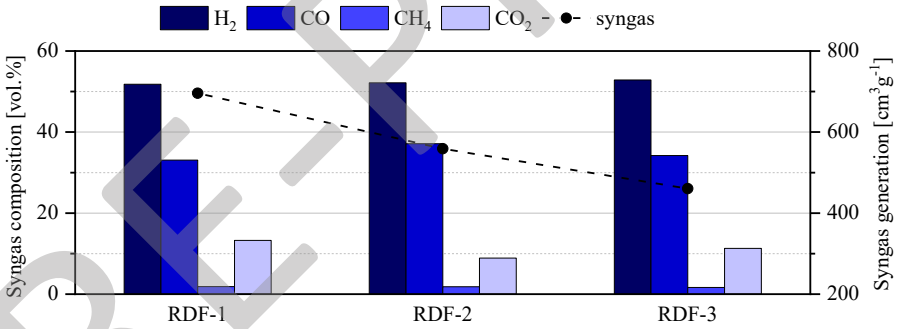

Figure 7

Quantity and composition of synthesis gas as a function of RDF composition

Approximately 89.4–94.0 vol% of the gases were identified. The effect of the initial RDF composition on gas production was less significant compared to its influence on the gas composition during pyrolysis. The analyzed syngas contained 47.1–48.7 vol.% H_2, 30.6–34.6 vol.% CO, 1.5–2.1 vol.% CH_4, and 9.1–10.2 vol.% CO_2. The total CO and H_2 contents, which are crucial components for further utilization in the chemical industry, varied between 77.8 and 83.3 vol%.

4. CONCLUSION

The utilization of municipal solid waste through thermochemical methods often encounters challenges due to its highly heterogeneous composition, influenced by various factors such as location, climate, and living standards. However, the conversion of this waste into refuse-derived fuel (RDF) offers a more manageable and uniform form for processing. Through appropriate high-treatment methods, the inherent unpredictability of RDF can be significantly reduced. Steam gasification presents a versatile approach, offering two potential directions depending on the desired end product: activated carbon or synthesis gas. This study focused on investigating the feasibility of preparing activated carbon from RDF and assessing the influence of RDF composition on product properties. The findings indicate that, within the examined compositional range, the produced chars exhibited approximately half the efficiency in phenol removal compared to high-quality commercial activated carbon. An increasing plastic content in the RDF mixture correlated with higher carbon content and adsorptivity of the activated carbons. Analysis of by-product gases produced after the pyrolysis process revealed minor fluctuations in syngas composition, with at least 77.8 vol.% total H_2 and CO content. These results are promising, considering that even if double the amount of these activated carbons is required, it can still be cost-efficient, given that the raw material is waste requiring treatment regardless.

ACKNOWLEDGMENTS

We acknowledge the support of the CIRCLETECH project (101079354) funded by the Horizon Europe programme of the European Commission.

REFERENCES

Adeniyi, A.G., Iwuozor, K.O., Emenike, E.C., Ajala, O.J., Ogunniyi, S., Muritala, K.B., 2024. Thermochemical co-conversion of biomass-plastic waste to biochar: a review. Green Chem. Eng. 5, 31–49. https://doi.org/10.1016/j.gce.2023.03.002

Bläker, C., Muthmann, J., Pasel, C., Bathen, D., 2019. Characterization of Activated Carbon Adsorbents – State of the Art and Novel Approaches. ChemBioEng Rev. 6, 119–138. https://doi.org/10.1002/cben.201900008

Cunha, F.S., Aguiar, A.P., 2014. Methods for the Removal of Phenolic Derivatives from Aqueous Effluents. Rev. Virtual Quím. 6. https://doi.org/10.5935/1984-6835.20140052

Das, D., Masek, O., Paul, M.C., 2024. Development of novel form-stable PCM-biochar composites and detailed characterization of their morphological, chemical and thermal properties. J. Energy Storage 84, 110995. https://doi.org/10.1016/j.est.2024.110995

Heidarinejad, Z., Dehghani, M.H., Heidari, M., Javedan, G., Ali, I., Sillanpää, M., 2020. Methods for preparation and activation of activated carbon: a review. Environ. Chem. Lett. 18, 393–415. https://doi.org/10.1007/s10311-019-00955-0

Hernández-Fernández, J., Lopez-Martinez, J., Barceló, D., 2021. Quantification and elimination of substituted synthetic phenols and volatile organic compounds in the wastewater treatment plant during the production of industrial scale polypropylene. Chemosphere 263, 128027. https://doi.org/10.1016/j.chemosphere.2020.128027

Ke, P., Zeng, D., Wang, R., Cui, J., Li, X., Fu, Y., 2022. Magnetic carbon microspheres as a reusable catalyst in heterogeneous Fenton system for the efficient degradation of phenol in wastewater. Colloids Surf. Physicochem. Eng. Asp. 638, 128265. https://doi.org/10.1016/j.colsurfa.2022.128265

Ladányi, R., 2015. Hejőpapi mechanikai-optikai előkezelő mű.

Liu, B., Han, B., Liang, X., Liu, Y., 2024. Hydrogen production from municipal solid waste: Potential prediction and environmental impact analysis. Int. J. Hydrog. Energy 52, 1445–1456. https://doi.org/10.1016/j.ijhydene.2023.11.027

Sebe, E., Nagy, G., Kállay, A.A., 2024. Steam gasification of char derived from refuse-derived fuel pyrolysis: adsorption behaviour in phenol solutions. Environ. Technol. 45, 5025–5036. https://doi.org/10.1080/09593330.2023.2283794

Thapar Kapoor, R., Treichel, H., Shah, M.P. (Eds.), 2021. Biochar and its Application in Bioremediation. Springer Nature Singapore, Singapore. https://doi.org/10.1007/978-981-16-4059-9

Wang, Q., Shi, Y., Zhao, Y., Ning, P., 2022. Design of solvent mixtures for removal of phenol from wastewater using a non-linear programming model with a multi-start method. Emerg. Contam. 8, 39–45. https://doi.org/10.1016/j.emcon.2021.11.001

Xayachak, T., Haque, N., Parthasarathy, R., King, S., Emami, N., Lau, D., Pramanik, B.K., 2022. Pyrolysis for plastic waste management: An engineering perspective. J. Environ. Chem. Eng. 10, 108865. https://doi.org/10.1016/j.jece.2022.108865